RSC Advances

PAPER

View Article Online
View Journal | View Issue

Cite this: *RSC Adv.*, 2025, **15**, 49584

Multi-functionalized biologically active isatin-tagged dihydropyrimidine derivatives: green synthesis by the use of recyclable Fe-dopped Ce-oxide nanoparticles, computational studies and *ex vivo* cytotoxic activity against breast cancer cells

Keshav Kumar Saini,[ab] Ravindra Kumar Upadhyay,[ac] Diksha Rani,[d] Smaranjot Kaur,[d] Ravi Kant,[e] Sanjay Kumar Dey*[d] and Rakesh Kumar *[a]

Received 25th September 2025
Accepted 9th November 2025

DOI: 10.1039/d5ra07279d

rsc.li/rsc-advances

A new class of compounds was designed and synthesised using a molecular hybridisation technique based on the dihydropyridine, isatin, triazole, thiazole, benzothiazole, and glucose scaffolds. The alkyne derivatives of dihydropyridine were synthesised by using reusable Fe-doped Ce-oxide nanoparticles *via* a three-component Biginelli reaction. The substances were then tested for their cytotoxic effects on two human breast tumour cell lines, MCF-7 and MDA-MB-231, as well as non-cancerous breast epithelial cell lines (*i.e.*, HEK293). The primary objective was to synthesise the more efficient breast cancer cell inhibitory molecules, which contain multiple scaffolds, and to investigate their potential as anti-breast cancer cell inhibitory therapeutic agents. Notably, compound-**6**, **7** and **14a** exhibited remarkable anti-cancer activity against two prominent breast-cancer cell-lines, MCF-7 and MDA-MB-231. The IC_{50} values of the compounds **6**, **7**, and **14a** against MCF-7 and MDA-MB-231breast cancer cell lines were found to be the lowest. The successful synthesis of these dihyropyrimidines using an environmentally friendly approach emphasises the significance of sustainable and eco-friendly methodologies in pharmaceutical research.

Introduction

Today, breast cancer is the most common disease and the second most prevalent cause of cancer death among women.[1] Many commercially available anti-breast cancer medications, such as alpelisib, anastrozole, cyclophosphamide, docetaxel, and tamoxifen citrate, are used to treat breast cancer (Fig. 1). Drug resistance to cancer chemotherapeutic agents is a profound medical issue. Moreover, many breast cancer patients are non-responsive or non-tolerant to most of the commercially available anti-breast cancer drugs.[2] As a result, there is a pressing need to design hybrid chemotherapeutic medication with multiple modes of action in a single molecule, apart from exploiting novel targets. These merged pharmacophores may address the active sites of many targets and provide a way to overcome drug resistance. The design of procedures with the lowest environmental impact is another significant element of modern organic synthetic methodology.[3] The use of one-time catalysts (metallic, acidic, and basic) and organic solvents is the primary source of environmental pollution.[4] The development of a new efficient and environment friendly improved process in organic synthesis is a need of the hour. In the past few years, carrying out organic reactions using new recyclable and waste-derived catalysts in green solvents has gained popularity due to environmental concerns.[5,6] One-pot cascade reactions are preferred over conventional methods since they are simple, quick, efficient, highly selective, give higher yields, maintain good atom economy, involve minimum steps, and eliminate waste production.[7] Biginelli reaction is a three-component reaction and it has received a lot of attention in the last few years because a variety of catalysts have been found that enable the synthesis of the resulting dihydropyrimidines (DHPMs) with exceptional yield, in contrast to the inconsistent performance observed in the early studies.[8] The Biginelli reaction is a one-pot condensation reaction with three components, which produces biologically active dihyropyrimidine by using β-keto esters, aldehydes, and urea/thiourea.[9] Several one-pot strategies for synthesising DHPM derivatives have been documented over the past decade, and several modifications have also been established to enhance the

[a]*Bioorganic Laboratory, Department of Chemistry, University of Delhi, Delhi-110007, India. E-mail: rakeshkp@email.com; Tel: +91 9810348999*

[b]*Department of Chemistry, Dyal Singh College, University of Delhi, India*

[c]*Department of Chemistry, Sri Venkateswara College, University of Delhi, New Delhi 110021, India*

[d]*Laboratory for Membrane Proteins and Structural Biology, Dr B. R. Ambedkar Center for Biomedical Research (ACBR), University of Delhi, Delhi-110007, India. E-mail: sdey@acbr.du.ac.in; Tel: +91 9205337595*

[e]*Department of Chemistry, Government Post Graduate College, G.B. Nagar, Noida, UP 201301, India*

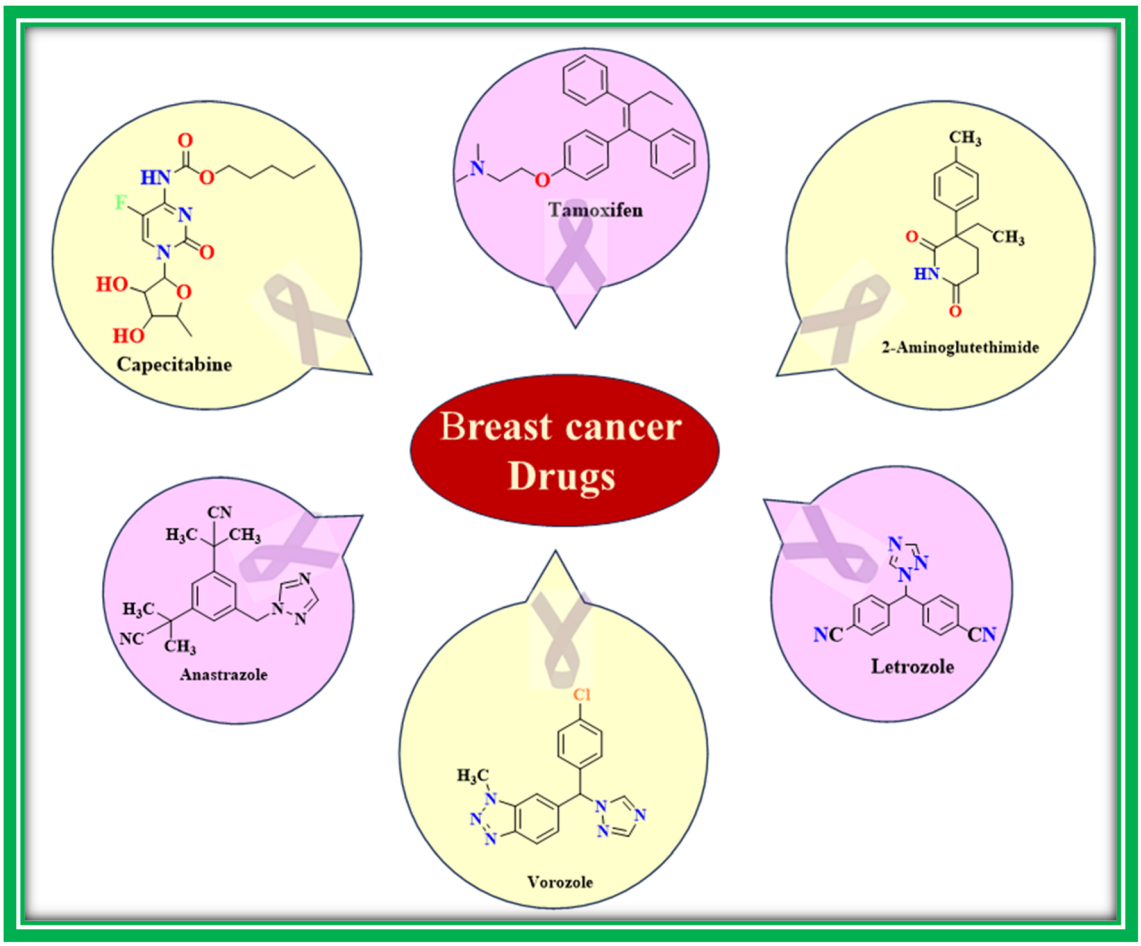

Fig. 1 Structures of some commercially available anti-cancer drugs.

yield and efficiency of the reaction. These modifications involved the use of Brønsted acids, Lewis acids, nanoparticles, mixed metal or metal oxide nanoparticles, ionic liquids, visible light photocatalysts, microwave assistance, clay, organic polymers, biocatalysts, ultrasound-irradiation, zeolites, and organic-inorganic mesoporous materials, *etc.*[10]

Dihydropyrimidines (DHPMs) have a variety of pharmacological properties, mainly anti-HIV,[11] calcium channel blocker,[12] anticonvulsant,[13] anti-fungal,[14] anti-tubercular,[15] antibacterial,[16] anti-cancer,[17] antihyperglycemic,[18] antihypertensive,[19] analgesic,[20] and antioxidant.[21] They are essential for the production of both RNA and DNA and are an essential component for regulating the cell lifecycle.

In synthetic organic chemistry, isatin plays an invaluable key role. It is one of the most important building block and a physiologically active pharmacophore that has been demonstrated to possess a variety of biological properties, including anti-cancer,[22] anti-fungal,[23] antibacterial,[24] antimicrobial,[25] anti-tubercular,[26] and anti-HIV[27] *etc.*

Single-drug, multi-target is a new emerging research field that has gained a lot of attention in recent years among the research community. This has been proven to be a powerful tool against complex diseases and drug resistance.[28] Molecular hybridization is an important strategy for the synthesis of single drug with enhanced biological features. In which two or more biologically active moieties are linked to enhance the efficiency of the drug. Triazoles are important linkers to link more than one scaffold,[29] which itself possesses a wide range of biological activities.[30] The 1,6-dihydropyrimidine, isatin, thiazole/benzothiazole, and 1,2,3-triazole rings are the basis for many clinically approved and under-trial medications with strong antifungal properties, in addition to the aforementioned claims. This makes the 1,6-dihydropyrimidine, isatin, thiazole/benzothiazole, and 1,2,3-triazole core an intriguing and little-studied pharmacophore.[31,32] During transcription, topoisomerase-II alpha, a naturally occurring enzyme, regulates and modifies the topologic properties of DNA.[33] Chromosome condensation, chromatid separation, and the alleviation of torsional stress during DNA replication and transcription are among the functions of this nuclear enzyme. It catalyses the temporary separation and reunification of two duplex DNA strands, allowing each strand to flow past each other and changing the DNA's structure. There are two variations of this enzyme that are most likely the result of a gene duplication. Drug resistance has been linked to a number of gene alterations, and the gene encoding this enzyme is the target of multiple anticancer drugs.[34] Targeting topoisomerase can cause damage to DNA, interfere with DNA replication, and eventually

cause cellular death or stop the proliferation of cancer cells. Topoisomerases are appropriate targets for therapeutic interventions because of their increased activity in cancer cells.[35]

Although there are drugs available like tamoxifen,[36] trastuzumab,[37] and paclitaxel.[38] There is still a need for new and improved drugs because (a) existing drugs develop resistance; (b) there are several subtypes of breast cancer, and all of them need to be targeted; and (c) various side effects have been observed for existing drugs.[39]

In this study, the new hybrids have been designed by combining thiazole/benzothiazole fused 1,6-dihydropyrimidine, isatin, and 1,2,3-triazole scaffolds into a single target molecule, continuing the strong interest in creating a single medication with multiple targets. One glucose derivative of each series was also prepared in order to check and enhance the solubility of the target compound. The utility of recyclable Fe-doped Ce-oxide nanoparticles as a catalyst in the Biginelli reaction was investigated at ambient temperature with the goal of developing an eco-friendlier procedure for the synthesis of dihydropyrimidine derivatives **6** and **7**, which further react with corresponding isatin azide derivatives to give target compounds **14a–d**, **15**, **16a–d** and **17**. To the best of our knowledge, the use of recyclable Fe doped Ce-oxide nanoparticles in green solvents like ethanol for the Biginelli reaction has not been reported previously. HEK-293, MDA-MB-231 and MCF-7 were the three cell lines used to screen the synthesised compounds in order to determine their breast cancer cell inhibitory potential. Utilising both MCF-7 and MDA-MB-231 cell-lines enables us to evaluate the synthesised compound's efficacy against various forms of breast cancer. It provides a broader perspective on how the compounds might be efficacious in various breast cancer subtypes, enabling researchers to identify potential compounds with broader applicability. These compounds can be potential drug candidates for targeting breast cancer and may have better efficacy than the existing ones.

On the basis of literature survey the new hybrids have been designed by combining thiazole/benzothiazole fused 1,6-dihydropyrimidine, isatin, 1,2,3-triazole and glucose scaffolds by molecular hybridisation into a single target molecule, this continues our keen interest in designing a single drug containing moieties that individually show anticancer activity.

Experimental procedure for chemical synthesis

Method of preparation

The target compounds that were synthesised had three biologically active scaffolds, namely (i) thiazole/benzothiazole-fused 1,6-dihydropyrimidine, (ii) a substituted isatin moiety and (iii) triazole. Triazole-threaded thiazole/benzothiazole-fused dihydropyrimidine and isatin were synthesised in eight steps. In order to synthesise the target molecules **14a–d**, **15**, **16a–d**, and **17**, the following synthetic process was used:

In step 1, Fe-doped nanoparticles have been prepared using the method described in the literature.[40] 15% $FeCl_3$ in ethanol (w/w) was added to a solution of $Ce(NO_3)_3 \cdot 6H_2O$ in ethanol and toluene (1 : 1). The ethanol-based oxalic acid solution is then added to the reaction mixture. An orange-coloured solution was formed, which was dried in a muffle furnace to get red-coloured Fe doped Ce-oxide nanoparticles (Scheme 1). These nanoparticles were further used for the synthesis of compounds **6** and **7** (Scheme 4).

In step 2, ethyl 4-chloroacetoacetate was converted to its alkyne derivative, ethyl-3-oxo-4-(prop-2-yn-1-yloxy) butanoate (**2**) by treating ethyl-4-chloroacetoacetate (**1**) with propargyl alcohol in the presence of NaH and in THF (Scheme 2).

With the aim of developing a more efficient and eco-friendly procedure for the Beginili reaction, in step 3, recyclable Fe doped Ce-oxide nanoparticles have been used for the synthesis of reactants **6** and **7** (Scheme 4). First of all, reaction conditions were screened to determine the appropriate solvents and the mole ratio of reactants for the targeted Beginili multicomponent reaction. With the goal of maximising the product yield in a relatively brief time frame, the reaction's optimisation was investigated for the synthesis of compound **6** using catalyst-free conditions and with a catalyst (Scheme 3) in a variety of solvents. It has been observed that no reaction was observed in solvent-less conditions or in polar aprotic solvents (ACN and THF). Imine is formed from the reaction of an aldehyde and 2-aminobenzothiazole. However, compound **6** was formed when CH_3OH and C_2H_5OH were used as solvents in the presence of catalyst, Fe doped Ce-Oxide nanoparticles on heating for 24 h at 30 °C (Scheme 3).

Further reaction conditions were optimised by carrying out reactions with Fe doped Ce-oxide nanoparticles at various

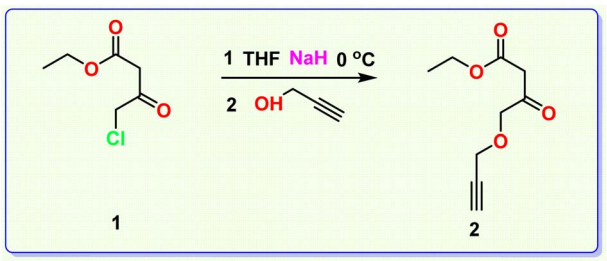

Scheme 2 Synthesis of ethyl 3-oxo-4-(prop-2-yn-1-yloxy) butanoate.

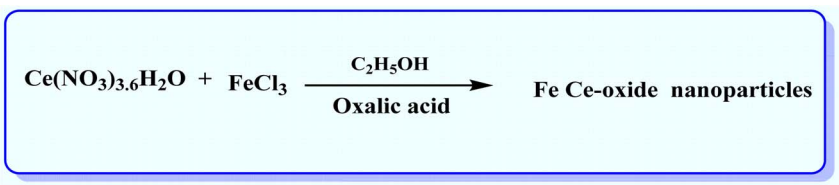

Scheme 1 Preparation of Fe doped Ce-Oxide nanoparticles.

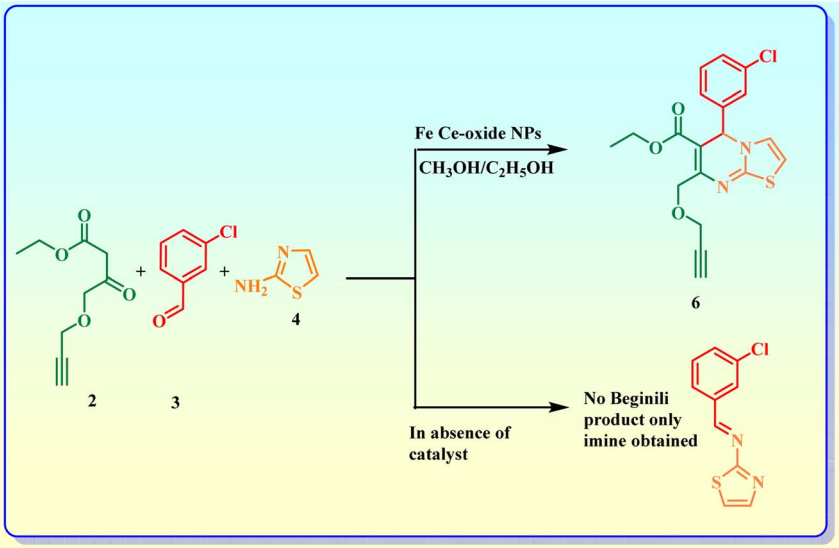

Scheme 3 Optimisation reaction conditions for the synthesis of compound **6** at 30 °C for 24 h.

temperatures to get maximum yield. It was observed that the maximum yield observed at 70 °C (Table 1). Heating the reaction mixture beyond 70 °C temperature gave side products along with the product.

To the solution of propargylated ethyl 4-chloroacetoacetate **(2)**, 3-chlorobenzaldehyde **(3)** and 2-aminothiazole **(4)**, were dissolved in C_2H_5OH. Novel starting material **6** was obtained by adding 0.05 M% Fe-doped Ce oxide nanoparticle in ethanol and refluxing the reaction liquid for eight hours., *via* a one-pot cascade reaction as shown in (Scheme 4). Likewise, after refluxing compounds 2, 3, and 5 in ethanol for eight hours with catalyst, compound 7 was produced.

Since synthesised compounds **6** and 7 are novel, to check the efficiency of nanoparticles in practice, compounds **6** and 7 were also synthesised by the reported method[41] *i.e.*, using conc. HCl in methanol by refluxing for 10 h. It was observed that the yield of Fe doped Ce-oxide nanoparticle-catalysed reactions was quite higher than that of acid-catalysed reactions as listed in Table 2.

In step 4, azide derivatives of acyl-protected D-glucose **(13)** and isatin **(10a–d)** and were prepared using the procedure described in the litrature[42,43] as illustrated in Schemes 5 and 6.

In step 5, compound **6** was reacted with various substituted azides **10a–d** and **13** to form 1,2,3-triazole derivatives **14a–d** and **15**, respectively *via* [2 + 3] cycloaddition reactions using DMF at 60 °C using a catalytic quantity of sodium ascorbate and $CuSO_4 \cdot 5H_2O$ (Scheme 7).

Similarly, compounds **16a–d** and **17** were synthesised by the click reaction of compound 7 with **10a–d** and **13**, respectively (Scheme 8).

Table 1 Reaction conditions are optimised for the synthesis of starting compound **6** in methanol and in ethanol at different temperatures

S. no.	Catalyst	Temperature	Yield in methanol	Yield in ethanol
1	Fe doped Ce-oxide NPs	10 °C	No reaction	No reaction
2	Fe doped Ce-oxide NPs	30 °C	30%	32%
3	Fe doped Ce-oxide NPs	50 °C	52%	55%
4	Fe doped Ce-oxide NPs	70 °C	88%	91%
5	Fe doped Ce-oxide NPs	80 °C	88%	91%

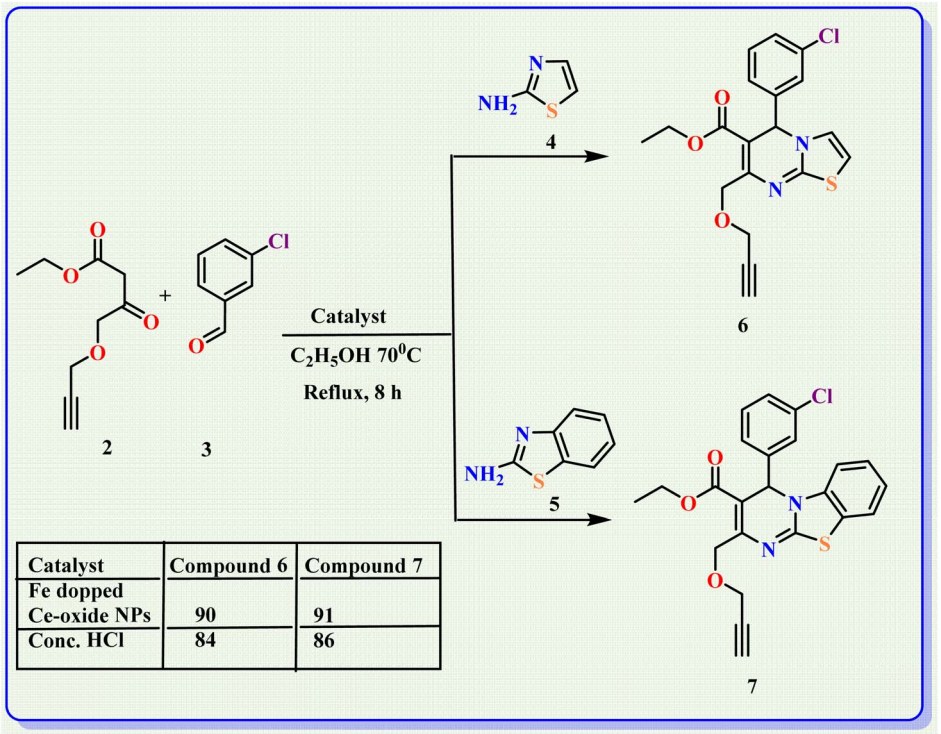

Scheme 4 Synthesis, of alkyne derivatives of thiazole and benzothiazole-based dihydropyrimidine **6** and **7**, respectively, using Fe doped Ce-oxide nanoparticles in C_2H_5OH.

Table 2 Yields comparison of compounds **6** and **7** in Fe doped Ce-oxide nanoparticle catalysed reactions and acid-catalysed reactions

S. no.	Compound	Yield with Fe doped Ce-oxide nanoparticles in ethanol, reflux 8 h	Yield with conc. HCl in methanol, reflux 10 h
1	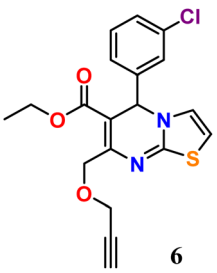 **6**	90%	84%
2	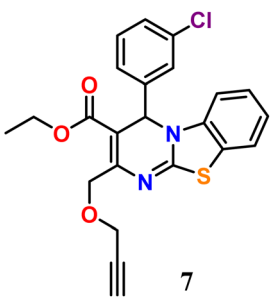 **7**	91%	86%

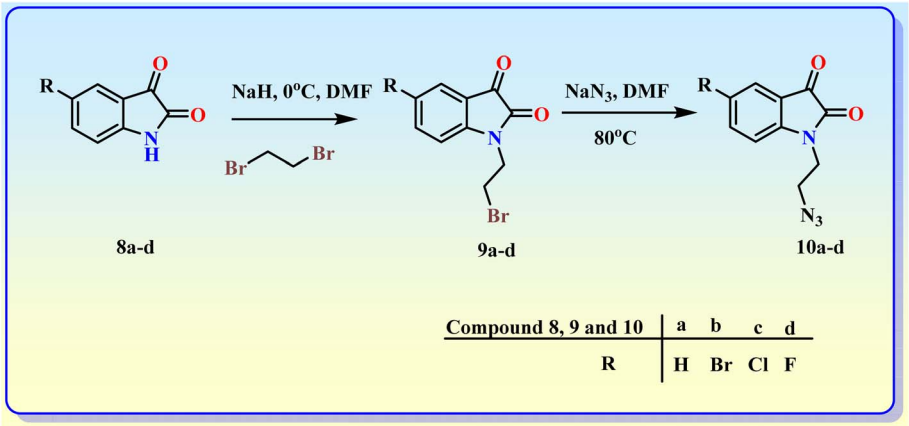

Scheme 5 Synthesis of *N*-(2-azidoethyl) isatin derivatives (**10a–d**).

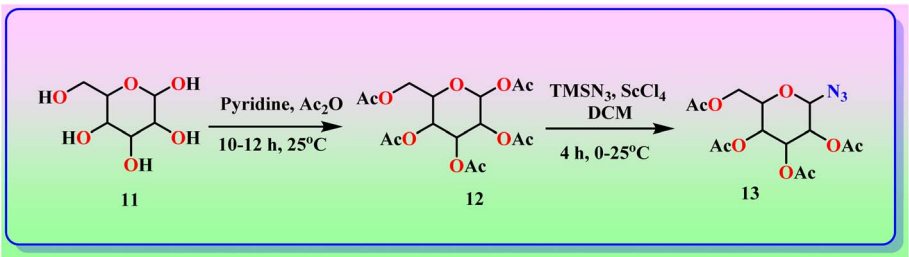

Scheme 6 Synthesis of azido derivative of acyl-protected D-glucose (**13**).

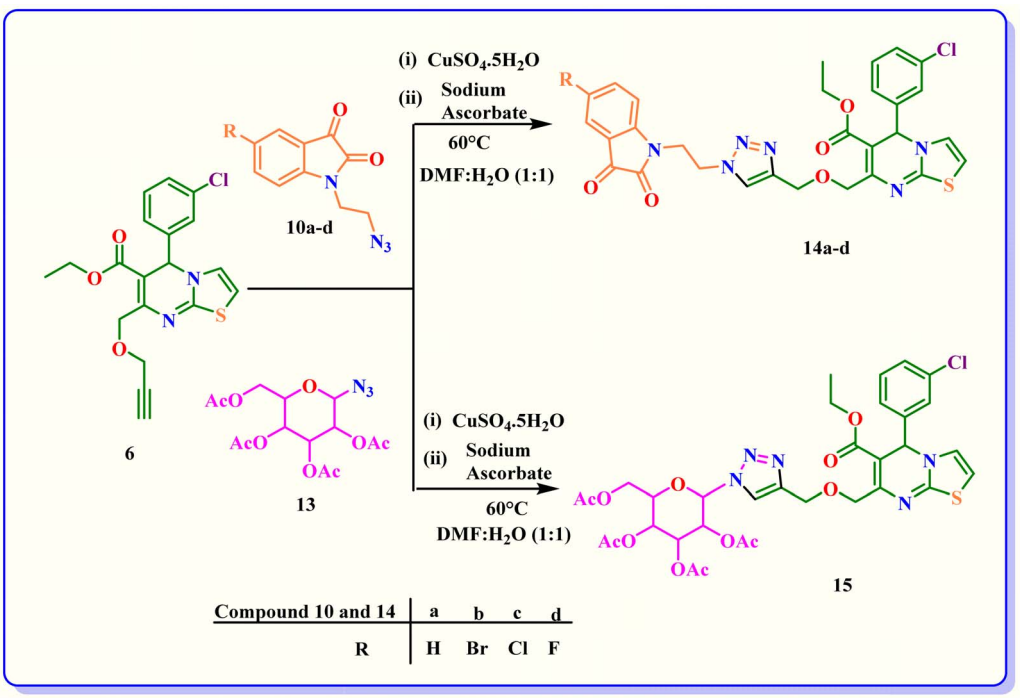

Scheme 7 Synthesis of novel 1, 2, 3- triazole derivatives of thiazole-fused dihydropyrimidines **14a–d** and **15**.

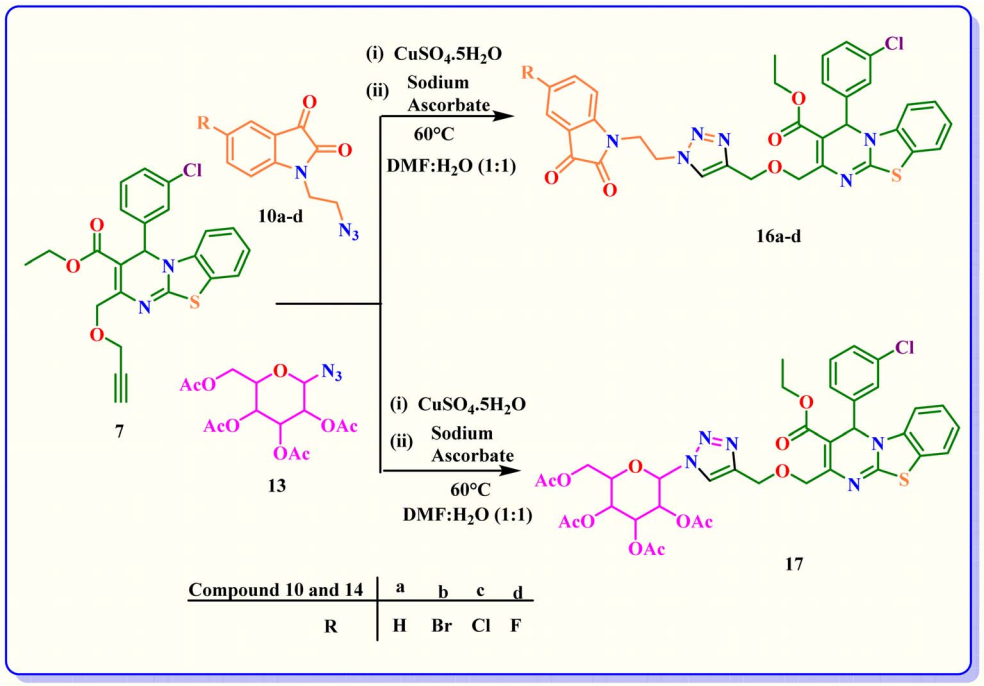

Scheme 8 Synthesis of 1, 2, 3- triazole derivatives of benzothiazole-fused dihydropyrimidine **16a–d** and **17**.

Results and discussions for chemical synthesis

The structures of all the synthesised compounds were validated using standard analytical techniques, including ^{1}H and ^{13}C nuclear magnetic resonance (NMR), infrared spectra (IR) and HRMS (high resolution mass spectrum) data. A triplet was detected at δ 1.21 ppm for three protons of the CH_3 group of the ethyl ester in compound **7**'s ^{1}H NMR. In the ^{1}H NMR of compound **7**, a triplet was observed at δ 1.21 ppm for three protons of the CH_3 group of the ethyl ester. A triplet was observed at δ 3.43 ppm for 1 proton of the terminal alkyne. A singlet was observed at δ 6.56 ppm for 1 proton of the dihydropyrimidine ring. Compound **6**'s^{13}C NMR spectra showed a peak at δ 164.77 ppm, which was attributed to the ester group's C=O carbon. The terminal alkyne carbon was identified as the source of a peak seen at δ 77.25 ppm. The peak that corresponds to the carbon of the ethyl ester's CH_3 group is evident at δ 13.98 ppm. Further HRMS (high-resolution mass spectrum) peak for the m/z $[M + H]^+$ ion peak appeared at 439.0942, which supports the synthesis of the compound **7** with the molecular formula $C_{23}H_{17}ClN_2O_3S$.

Compound **14a**'s ^{1}H NMR revealed a triplet for the ester CH_3 group's three protons at δ 1.08 ppm. A singlet for the dihydropyrimidine ring's single proton was detected at δ 6.37 ppm. A singlet for a single proton of the 1,2,3-triazole ring was identified at δ 8.19 ppm. The compound **14a**'s^{13}C NMR spectra identified a peak at δ 182.93 ppm, which was attributed to the carbonyl carbon on the isatin ring's C-3 position. The peak that showed up at δ 165.26 ppm was attributed to the ester group's C=O carbon. The triazole ring's C-4 carbon is responsible for the peak seen at δ 130.93 ppm. Further HRMS (high-resolution mass spectrum) peak for the m/z $[M + H]^+$ ion peak appeared at 605.1353, which supports the synthesis of the compound **14a** with the molecular formula $C_{29}H_{25}ClN_6O_5S$.

Methods for biological evaluation

Cell culture. MCF-7, MDA-MB-231, and HEK-293 cell lines used in this study were obtained as a kind gift from Dr Anant Narayan Bhatt. Cells were cultured in DMEM (Dulbecco's Modified Eagle's Medium, Gibco, St. Louis, USA) media supplemented with 10% FBS (Fetal Bovine Serum, Gibco, USA) and 1% Pen-Strep (penicillin–streptomycin, Gibco, USA) in a humidified CO_2 (5%) incubator at 37 °C. DMSO (Sigma Aldrich, USA) and PBS (Sigma Aldrich, USA) were used as vehicle control and solvent control respectively. Whereas tamoxifen (GLR Innovations, India; Cat no. GLR19.143958) was taken as a positive control with known anti-breast cancer activity.

***Ex-vivo* breast cancer cell growth inhibition activity screening against MCF-7 and MDA-MB-231 cells by MTT cell viability assay.** The synthesized compound series were screened for their breast cancer cell growth inhibition activity against MCF-7, and MDA-MB-231 while non-breast cancer HEK-293 cell line was used for screening the nonspecific effects and toxicity of compounds, if any. The adhesive cells were trypsinized to detach cells from matrix of the flask using 0.25% trypsin (Gibco; USA Cat no. 25200056) and 20 000 cells were seeded per well of 24 well flat bottom plates followed by incubation in CO_2 incubator at 37 °C for 20–24 h. The cells were treated with 100 μM concentration of compounds dissolved in DMEM media in triplicates along with the positive control drug (tamoxifen), vehicle control (DMSO), and solvent control (PBS) for 48 h.

Following incubation, cells were treated with MTT (3-(4,5-dimethylthiazol-2-yl)-2,5-diphenyltetrazolium bromide) (Sigma-Merck, USA) and incubated for 2 h at 37 °C in dark, then formazan granules were dissolved in DMSO with gentle shaking. The cell viability was evaluated by taking absorbance at 570 nm using a Tecan Multiplate Reader (SpectraMax® iD3

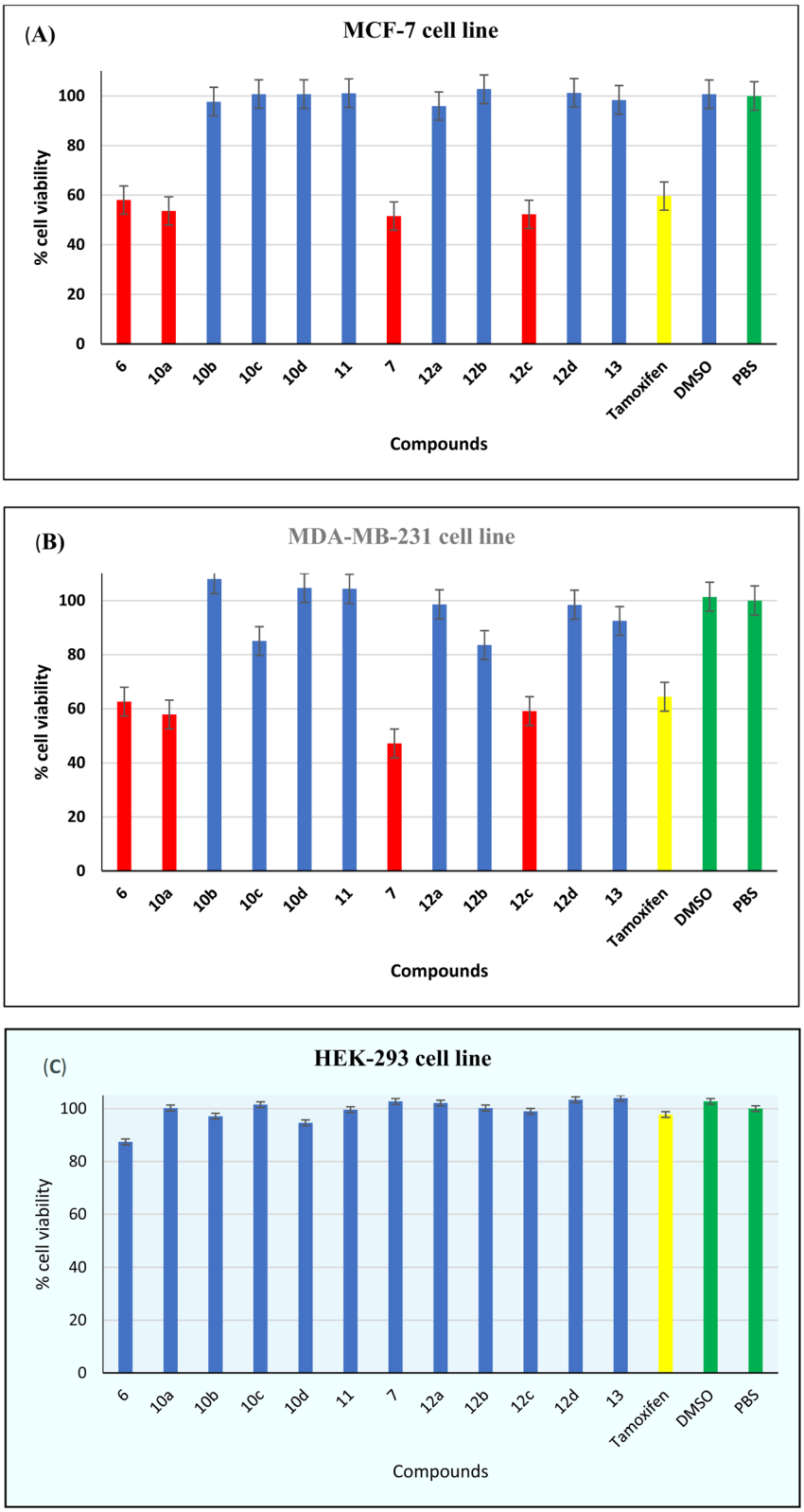

Fig. 2 Cell viability evaluation of cells treated with compounds: after 48 hours of treatment with 100 μM concentrations of the corresponding compounds, the viability of (A) MCF-7 cells, (B) MDA-MB-231 cells, and (C) HEK-293 cells was assessed using the MTT cell viability test.

multi-mode microplate reader). For titration of the best four compounds and calculation of IC_{50} against MCF-7 and MDA-MB-231 cells, further diluted stocks of 1 μM, 10 μM, and 100 μM were made in DMSO and treated in three replicates.

Molecular interaction studies. A small in-house chemical library of 12 compounds was produced, consisting of known moieties from FDA-approved anti-cancer/anti-breast cancer medications. A literature search was conducted to identify a protein that could serve as a potential breast cancer target. Human topoisomerase II alpha (PDB ID: 5GWK) was selected as a good candidate for this purpose. The crystal structure of topoisomerase II alpha (PDB ID: 5GWK) was downloaded from the Protein Data Bank in.pdb format. Protein preparation was carried out using the Protein Preparation Wizard in Maestro tool of Schrodinger. This included removal of water molecules beyond 5 Å of the binding site, assignment of bond orders, addition of missing hydrogens, optimization of hydrogen bonding, and energy minimization of the structure. The 2D

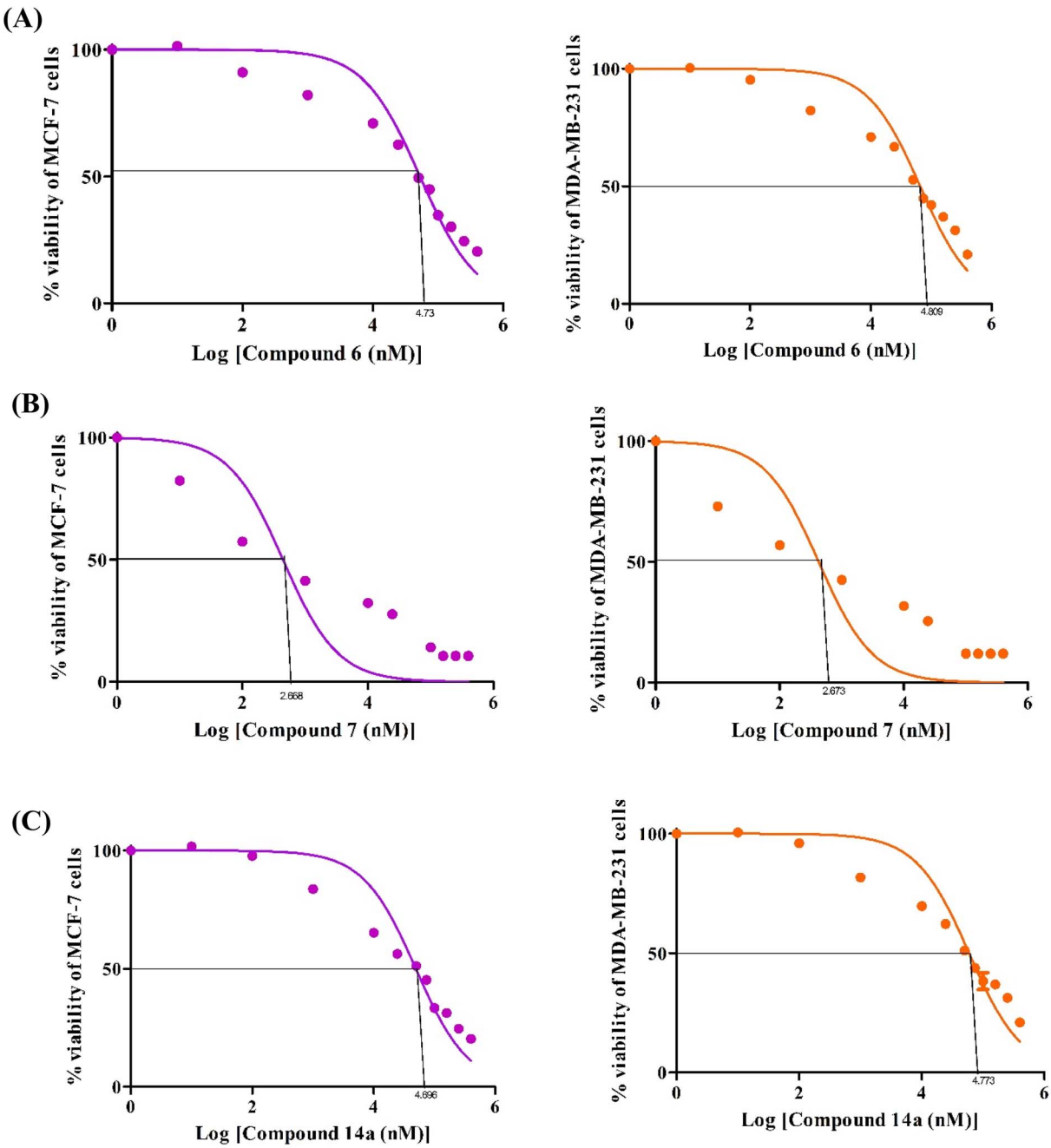

Fig. 3 IC_{50} plots of the best breast cancer cell growth inhibitors compounds **6**, **7** and **14a** evaluated against MCF-7 and MDA-MB-231 cells. (A) Compound **6**, (B) compound **7** and (C) compound **14a**. Each experiment was repeated thrice and the plots are showing the corresponding SD values. (compounds **6**, **14a**, and **7** showed IC_{50} values of 52.7 ± 0.73 μM, 42.3 ± 0.83 μM, and 63.7 ± 2.17 nM in MDA-MB-231 cells, and 62.6 ± 0.86 μM, 81.9 ± 2.26 μM, and 55.0 ± 1.19 nM in MCF-7 cells, respectively.).

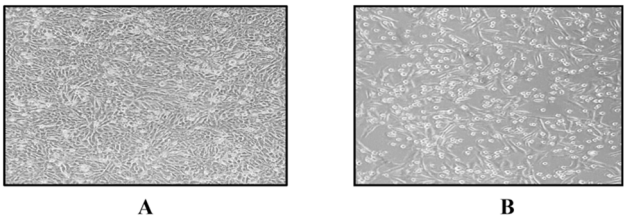

Fig. 4 Cells before compound/drug treatment. (A) MCF-7, a breast cancer cell line; (B) HEK-29, a human embryonic kidney cell line that serves as a non-cancerous control.

structures of the library compounds and tamoxifen were drawn using ChemDraw Pro 12.0 and saved in.sdf format. The ligands were converted into their 3D structures and optimized using the LigPrep tool in Schrodinger, ensuring proper stereochemistry and protonation states at pH 7.0 ± 2.0. A receptor grid was generated around the topoisomerase II alpha using the Glide Grid Generation tool, ligands were docked into the binding site of the prepared protein using the Glide module in standard precision (SP) mode for an initial screening, followed by extra precision (XP) docking for top-ranked compounds to refine binding poses and improve accuracy. Docked poses were ranked based on their Glide docking scores, which reflect the binding affinity of the ligand to the target protein. Lower (more negative) docking scores indicate stronger binding affinities. Docked poses were analyzed and visualized using Schrodinger's Maestro, PyMOL and Chimera 1.15 to inspect binding interactions, including hydrogen bonds, hydrophobic contacts, and pi-stacking interactions. Based on the docking scores, compounds were ranked, and top hits were identified as potential binders to topoisomerase II alpha.

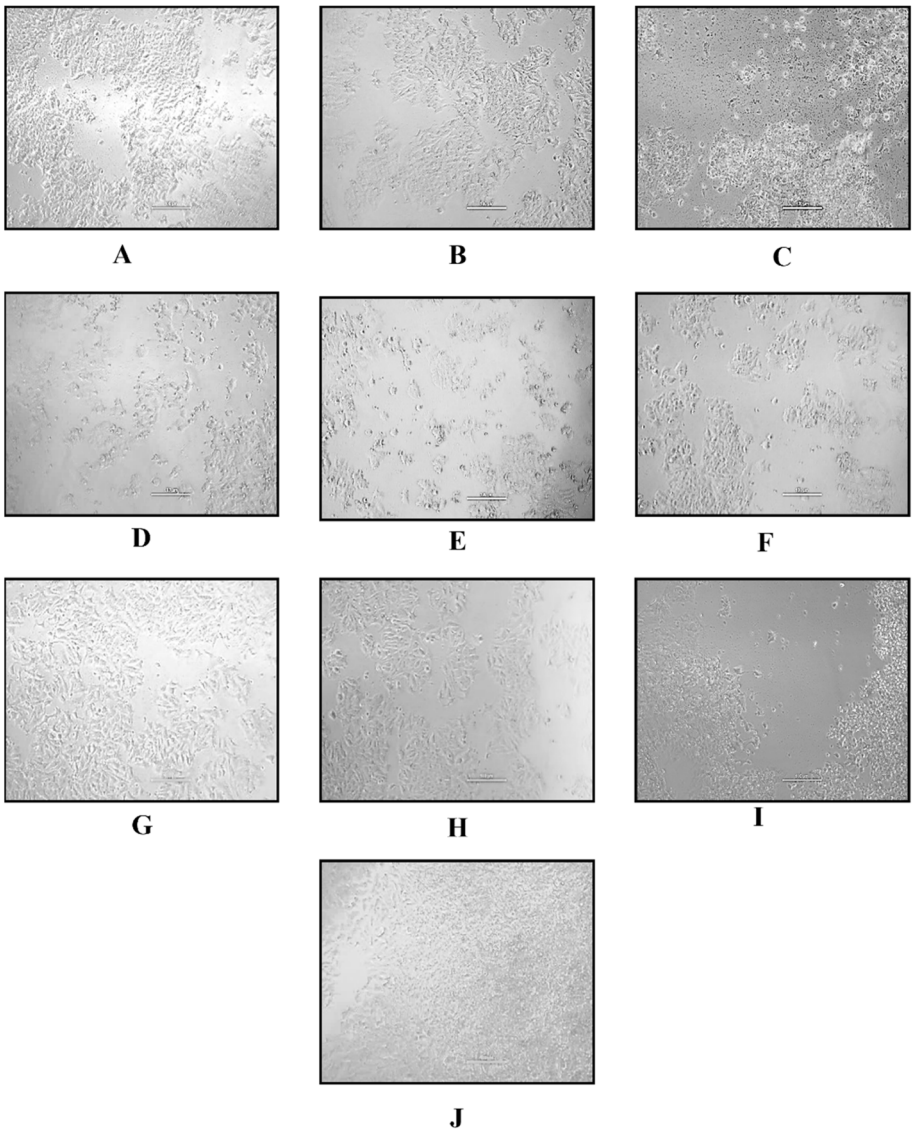

Fig. 5 Compounds inducing the breast cancer cell-selective cytotoxicity: MCF-7 cell-lines were treated for 48 hours with (A) **6**, (B) **14a**, (C) **7**, (D) **16c**, (E) **16d**, (F) tamoxifen (positive control), (G) PBS (solvent control), and (H) DMSO (vehicle control) (I) **16d** (J) **17** and Sections A to J indicative of a minimum of three separate tests.

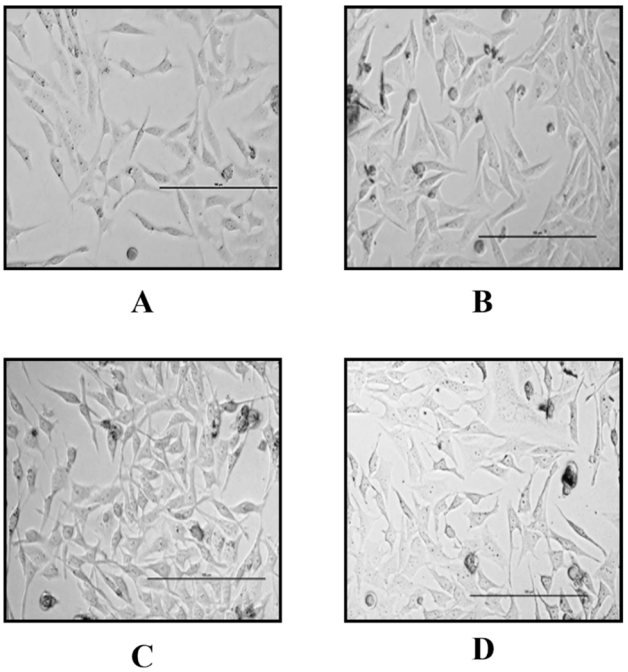

Fig. 6 MDA-MB-231 cell lines in representative pictures prior to compound/drug treatment.

Structure activity relationship (SAR) analysis. A completely integrated computational workflow utilizing cutting-edge tools from the Schrödinger software package was used to carry out the structure–activity relationship (SAR) research. The Glide module was used to perform molecular docking simulations in order to determine the binding affinities of the synthesized ligands within the target protein's active region. The QikProp and Canvas modules were used to calculate important physicochemical characteristics, such as molecular weight, *A* log *P*, hydrogen bond acceptors (HBA), hydrogen bond donors (HBD), rotatable bonds (RB), heavy atom count, polar surface area (PSA), and molar refractivity (MR). Comprehensive cheminformatics analysis, including the computation of several molecular descriptors, grouping, similarity evaluations, and data visualization, was made possible by the Canvas module in particular. This allowed for a thorough assessment of compound drug-likeness and structural variety. To find any parameter violations, all computed attributes were methodically evaluated in comparison to Lipinski's rule of five.[44]

Results and discussions for biological evaluation of the synthesized compounds

Functional evaluation of the synthesised compounds

Cancer cell growth inhibition activity using MTT cell viability assay. The MTT assay was used to examine the cell viability of MDA-MB-231, MCF-7, and HEK-293 cell lines in the presence of synthesised chemicals. Data showed that MDA-MB-231 and MCF-7 cells had poor cell viability when exposed to 100 μM dosages of the four compounds—**6**, **14a**, **7**, and **16c**—but that none of the chemicals tested were hazardous to HEK-293 at levels of up to 100 μM. The cell survival rate for compound **6** was 58%, whereas MCF-7 cells treated with chemicals at 100 μM, while compounds **14a**, **7**, and **16c** had ∼52% cell survival, which is efficacy-wise better than the known anti-breast cancer drug, tamoxifen.[45] In other words, compound **6** could kill 42% of MCF-7 cells at a dose of 100 μM. Similarly, **14a**, **7**, and **16c** are causing ∼48% of cell deaths at similar doses of 100 μM, while tamoxifen kills only 40% of the cells. Conversely, when chemicals were administered to MDA-MB-231 cells at a dosage of 100 μM, wells with **6** had 62% cell survival, **14a** had 58%, **7** had 48%, and **16c** had ∼58% cell survival, which is way better than the known anti-breast cancer drug tamoxifen, which has a cell survival of 63%. Alternatively, compound **6** might kill 38% of MDA-MB-231 cells at 100 μM. Likewise, compounds **14a**, **7**, and **16c** are causing ∼42%, 52% and 42% cell deaths at similar doses of 100 μM, while tamoxifen kills only 37% of cells. These

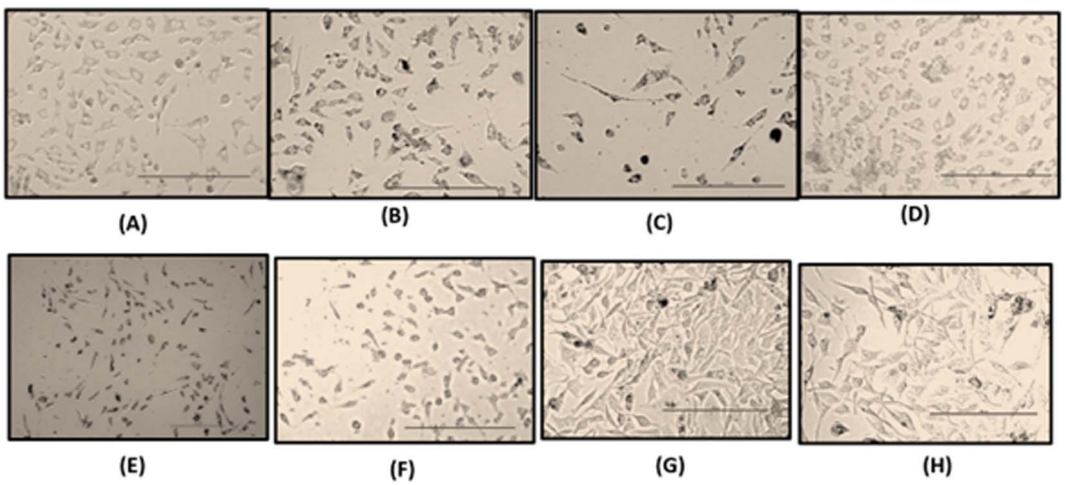

Fig. 7 MDA-MB-231 cells subsequent to compound/drug treatment. The cells MDA-MB-231 were exposed to (A) **6**, (B) **14a**, (C) **7**, (D) **16c**, (E) **16d**, (F) tamoxifen (positive control), (G) PBS (solvent control), and (H) DMSO (vehicle control) for 48 h.

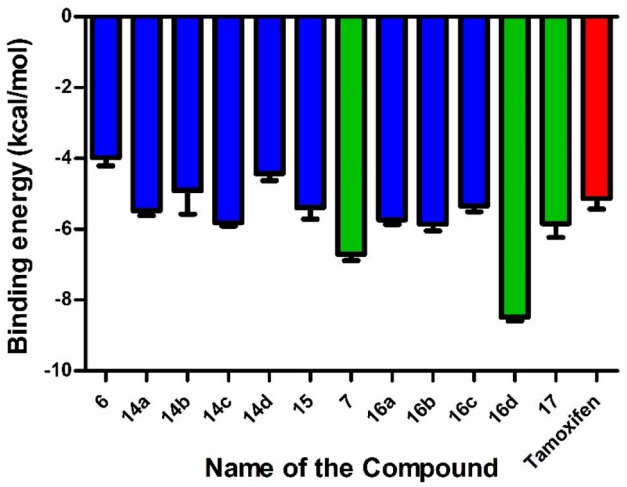

Fig. 8 Graph showing binding energies based on docking scores against topoisomerase II of 12 compounds (blue: less negative, green: more negative), and tamoxifen (red: negative control).

calculated results are shown in Fig. 2 below, as plotted by % cell viability *versus* compound numbers.

In order to determine the IC_{50} values, further investigation was conducted on four compounds (**6**, **14a**, **7**, and **16c**) by treating MDA-MB-231 and MCF-7 cell-lines with varying doses of the compounds. Compounds **6** and **14a** were tested from 10 nM to 100 μM, while compound **7** was tested in the dose range of 100 pM to 100 μM due to its potency even at low doses (Fig. 3A–C) However, the IC_{50} value of **16c** was found to be higher than >100 μM, indicating it is not a viable candidate for further research, and therefore, it was excluded from the plot. Based on the results presented in Fig. 3A–C, these results indicate that Compound 7 is the most effective compound with both MCF-7 and MDA-MB-231 cell-lines.

Microscopic analysis of cell morphology. The microscopic analysis was performed before and after compound/drug treatment using a Nikon microscope at 10× magnification. MCF-7 cells treated with compounds **6**, **7**, **14c**, and **14d** as well as tamoxifen, for 48 h have shown significant changes in their morphology, which can clearly be seen in photomicrographs shown in Fig. 5. Cellular shrinkage (Fig. 5C) and dead cells (Fig. 5F) were also seen after treatment in comparison to untreated cells. The untreated MCF-7 cells (Fig. 4A) and HEK-293 cells (Fig. 4B) were appeared healthy under the microscope, whereas the **14a**, **14c**, **15**, **16b**, **16c**, **12e** (Fig. 5A–F) treated MCF-7 cells are mostly dead and morphologically very different too from normal MCF-7 cells. There were no dead cells in the cells that were treated with solvent control PBS and vehicle control DMSO. Moreover, cells were growing and flourishing as normal in these wells (Fig. 5G and H in the SI). **14d** is not showing breast cancer cell growth inhibition, which is not affecting cells much. Whereas the cells treated with positive control tamoxifen were mostly dead as expected (Fig. 5I and J). Hence, these six compounds, namely, **14a**, **14c**, **15**, **16b**, **16c** and **17** have the highest breast cancer cell inhibitory activity out of all the compounds and have better cancer selective effect. These compounds inducing significant cell death and morphological changes in comparison to controls. Representative images of MDA-MB-231 cell-lines before and after treatment with compounds/drugs are shown in Fig. 6 and Fig. 7, respectively.

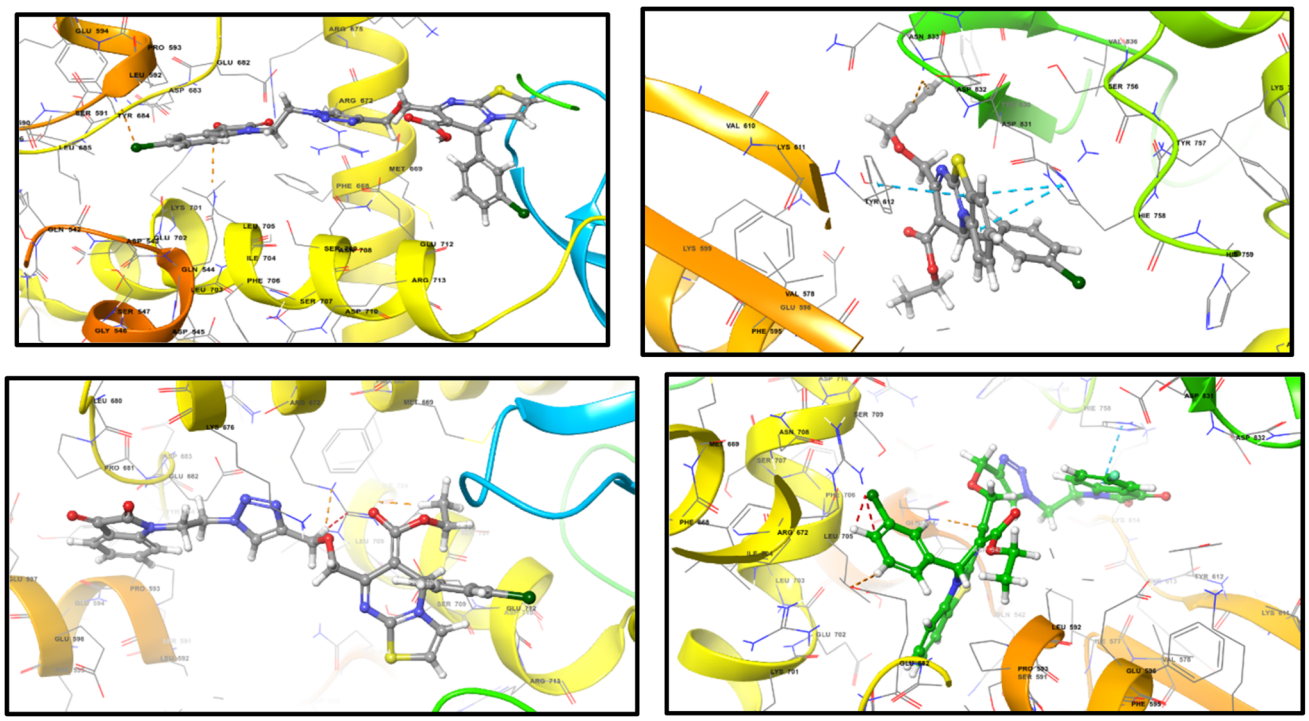

Fig. 9 Three dimensional docked structures of the best four compounds (**14c**, **7**, **16a** and **16d**) with topoisomerase (PDB ID: 5GWK) visualized using Maestro visualizer.

Binding studies by *in silico* methods. Utilising the Schrödinger, molecular interaction experiments were conducted against topoisomerase II alpha with a PDB ID 5GWK.[19] To determine if in-house drugs were effective in inhibiting topoisomerase II, an enzyme essential to cancer cell survival, molecular interaction experiments were carried out. The compounds were designed based on the known backbone that targets topoisomerase, and modifications were made to potentially enhance their efficacy.

Docking glide scores were obtained for two compounds **6** and **14d** indicating low efficacy as their binding score is around -4 kcal mol^{-1}. However, further analysis revealed that out of all the 10 compounds, **14a**, **14b**, **14c**, **15**, **7**, **16a**, **16b**, **16c**, **16d**, and **17** exhibited high efficacy, with binding scores ranging from approximately -5.02 to -8.28 kcal mol^{-1} (Fig. 8). Among these, **14c**, **7**, **16a** and **16d** showed the lowest binding energies (-5.77, -6.32, -5.67, and -8.28 kcal mol^{-1}, respectively), indicating a strong interaction with topoisomerase II alpha (Fig. 9 and 10).

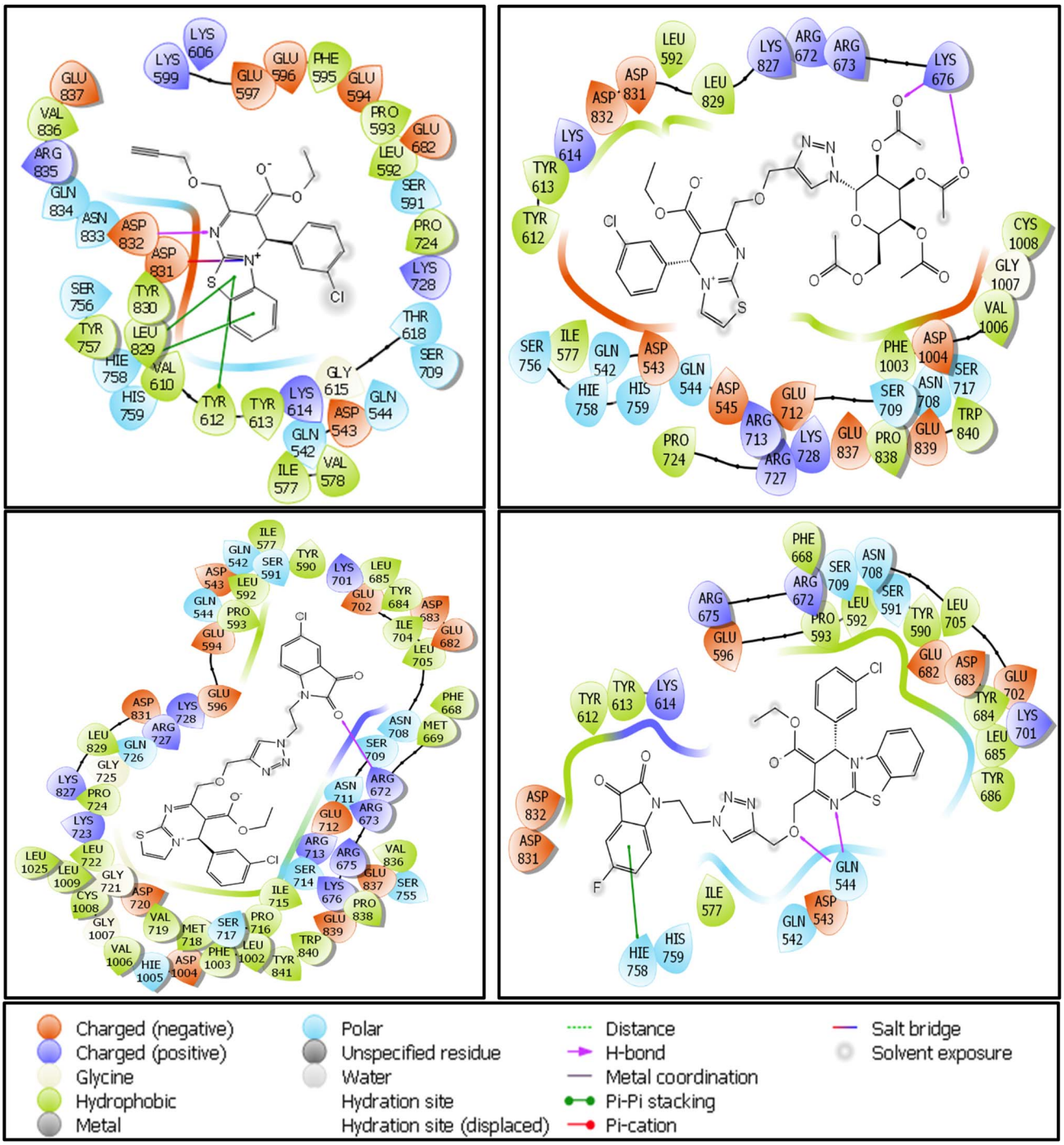

Fig. 10 Two-dimensional docked structures of the best four compounds (**14c**, **7**, **16a** and **16d**) with topoisomerase (PDB ID: 5GWK) visualised using Maestro visualizer.

Table 3 Structure–activity relationship (SAR) analysis of docked ligands[a]

S. no.	Compound	Docking score (kcal mol^{-1})	Predicted activity	MW (Da)	*A* log *P*	HBA	HBD	RB	Heavy atom	PSA (Å^2)	MR (cm^3 mol^{-1})	Polar (%)	Lipinski violations
1	**6**	−3.52	−0.08	388.87	3.69	3	1	6	26	86.00	95.89	44.54	None
2	**7**	−5.02	−0.14	438.93	5.45	3	1	6	30	86.00	111.60	52.89	*A* log *P* > 5
3	**14a**	−6.32	−0.17	605.06	3.12	7	0	10	42	154.09	154.54	70.25	MW > 500
4	**14b**	−5.17	−0.13	683.96	3.87	7	0	10	43	154.09	162.16	72.88	MW > 500
5	**14c**	−3.58	−0.12	639.51	3.78	7	0	10	43	154.09	159.34	72.22	MW > 500
6	**14d**	−5.78	−0.12	623.05	3.32	7	0	10	43	154.09	154.76	70.16	MW > 500
7	**15**	−4.03	−0.12	762.18	1.66	14	0	17	52	231.14	177.26	77.68	MW > 500, HBA > 10
8	**16a**	−5.68	−0.09	655.12	4.88	7	0	10	46	154.09	170.25	78.61	MW > 500
9	**16b**	−5.63	−0.10	734.02	5.63	7	0	10	47	154.09	177.87	81.24	MW > 500, *A* log *P* > 5
10	**16c**	−5.03	−0.11	689.57	5.55	7	0	10	47	154.09	175.05	80.58	MW > 500, *A* log *P* > 5
11	**16d**	−8.28	−0.14	673.11	5.09	7	0	10	47	154.09	170.46	78.52	MW > 500, *A* log *P* > 5
12	**17**	−5.14	−0.09	812.24	3.42	14	0	17	56	231.14	192.97	86.04	MW > 500, HBA > 10
13	Tamoxifen	−5.28	−0.12	371.51	6.32	1	0	8	28	12.47	119.26	56.02	*A* log *P* > 5

[a] MW: molecular weight, *A* log *P*: partition coefficient (log *P*, computationally predicted), HBA: hydrogen bond acceptors, HBD: hydrogen bond donors, RB: rotatable bonds, PSA: polar surface area, MR: molar refractivity.

The docking conformations of the protein structures (PDB ID 5GWK) with the compounds revealed that specific amino acids, including GLN-1095, THR-825, PHE-828, LYS-287, GLN-1049, ALA-588, ILE-574, LYS-821, and LEU-826, played a vital role in the binding process. Topoisomerase II alpha consists of several domains such as TOPORIM, WHD, TOWER, ATPase, and CTD, which contribute to functions like metal binding, DNA cleavage, and dimerization. Notably, the WHD and CTD domains are primarily involved in binding, with functions related to DNA intercalation and DNA cleavage (Table S1 in SI). Protein-ligand interacting amino acid residue details of compounds **7**, **14c**, **16a**, **16d** and the standard drug tamoxifen with topoisomerase II alpha using UCSF Chimera software are shown in Table S2 (in SI)

Table S1 (in the SI) provides a comprehensive illustration of the molecular interactions between the ligand molecules **6**, **7**, **14a–d**, **15**, **16a–d**, and **17** and different residues of various amino acids in the binding pocket of the enzyme topoisomerase II alpha.

Structure–activity relationship (SAR) of the compounds. A thorough assessment of the pharmacokinetic and effectiveness profiles of the synthesized compounds in breast cancer cell models is provided by the combined structure–activity relationship (SAR) and experimental IC_{50} analysis. Most of the analogs from the **14** and **16** series, along with compounds **15** and **17**, greatly exceeded the molecular weight limit suggested by Lipinski's rule of five. In many cases, they also exceeded permissible limits for hydrogen bond acceptors and lipophilicity. These variations point to possible oral bioavailability restrictions. Compounds **6** and **7**, on the other hand, showed more advantageous drug-like characteristics; compound **6** completely met all Lipinski criteria, while compound **7** just slightly increased *A* log *P* (5.45), Table 3. It's interesting to note that tamoxifen, a clinically proven treatment for breast cancer, also surpasses the Lipinski-specified *A* log *P* threshold, which may have an impact on its pharmacokinetic profile. Similar to tamoxifen, compound **7** exhibits significantly greater cytotoxic efficacy and considerable biological inhibition at concentrations far lower than those reported for tamoxifen under comparable experimental settings, although it only slightly exceeds the optimum *A* log *P* limit. The idea was that molecular structure of compound **7** provides strong target engagement and cellular efficacy without significantly compromising drug-likeness is thus supported by the SAR study. All things considered, these findings identify compound **7** as a very promising lead that successfully strikes a balance between favourable physicochemical characteristics and strong nanomolar cytotoxicity (63.7 ± 2.17 nM and 55.0 ± 1.19 nM), providing benefits over well-known clinical standards like tamoxifen.

Conclusion

This work involved the synthesis of a number of dihydropyrimidine derivatives using a greener, environment-friendly method using recyclable Fe-doped Ce-oxide nanoparticles in ethanol. The nanoparticles are recyclable and give excellent yields up to 5 cycles. Further novel isatin-linked triazole derivatives were synthesized by starting with dihydropyrimidine derivatives. All synthesized compounds were subjected to screening against human breast-cancer cell-lines *in vitro*. The results were encouraging, as these derivatives exhibited remarkable anti-cancer activity against two prominent breast-cancer cell-lines, MCF-7 and MDA-MB-231. The IC_{50} values of the compounds **6**, **14a**, and **7** were 52.7 ± 0.73 μM, 42.3 ± 0.83 μM, and 63.7 ± 2.17 nM, respectively against MDA-MB-321 cancer cell lines. In the case of MCF-7 cells, **6**, **14a**, and **7**

demonstrated IC_{50} values of 62.6 ± 0.86 μM, 81.9 ± 2.26 μM, and 55.0 ± 1.19 nM, respectively. These findings highlighted the significant potential of these dihydropyrimidine derivatives aseffective agents against breast cancer. This is especially true of compound **7**, which showed an incredibly low IC_{50} value of 63.7 ± 2.17 nM against MDA-MB-231 cells and 55.0 ± 1.19 nM against MCF-7 cells. In molecular interaction studies, intriguing results were obtained, indicating that compounds **14a**, **7**, **16b**, and **16d** exhibited the lowest binding scores. This suggested that by preventing the topoisomerase enzyme from performing its intended function, these compounds could be able to prevent breast cancer. Inhibition of this enzyme can impede the survival of cancer cells, consequently providing a potentially effective therapeutic strategy for breast cancer. These findings highlighted the possibility of utilising these compounds as effective therapeutic agents, warranting further exploration and investigation into their precise mechanisms of action. This study contributes to the growing body of knowledge in the area of breast cancer treatments and emphasises the significance of additional research into the pharmacological characteristics and modes of action associated with these compounds. These results provided a solid foundation for future studies aimed at developing these derivatives into promising anti-breast cancer drugs.

Author contributions

The notion was put out by KKS, who also created the manuscript portions. The final manuscript was written and reviewed by all of the writers. KKS, DR, and SJK conducted experiments, analysed data, and prepared the diagrams and tables. SKD and RS supervised the study and acquired funding for the study.

Conflicts of interest

The authors declare that none of the information in this study has any conflicts of interest. This work has been submitted for a patent with an Application no. 202411007373.

Data availability

Research data has been attached in the uploaded supplementary information (SI). Supplementary information is available. See DOI: https://doi.org/10.1039/d5ra07279d.

Acknowledgements

KKS is grateful to the Institutions of Eminence (IoE) for providing funds to carry out the present research work. KKS is also grateful to the USIC (University Science Instrumentation Centre), University of Delhi, for providing the required instrumentation facilities. SKD acknowledges financial and infrastructural support from the University of Delhi (R&D and seed grants) and Dr B. R. Ambedkar Centre for Biomedical Research [ACBR] (start-up and research grants). SKD also acknowledges the Institution of Eminence grant (grant ID: IoE/2021/12/FRP) from the University of Delhi, India; SERB-DST ANRF grant (CRG/2023/007380) and ICMR extramural grant (grant ID: 5/4/1-11/CVD/2022-NCD-I) for providing financial support for the current work. RKU acknowledges the fellowship support from CSIR. DR acknowledges her Junior Research fellowship from the DBT (grant ID: DBT/2021-22/CBR/1702), and SKJ acknowledges her Project Assistant fellowship from the ICMR (grant ID: 5/4/1-11/CVD/2022-NCD-I) to complete this work. The authors also gratefully acknowledge CSIR for financial support for this work.

References

1 X. B. Hong R, *Cancer Commun.*, 2022, **42**, 913–936.
2 G. P. Dailey, E. J. Crosby and Z. C. Hartman, *Cancer Gene Ther.*, 2023, **30**, 794–802.
3 S. Lakshmanan and N. Ramalakshmi, *Synth. Commun.*, 2016, **46**, 2045–2052.
4 E. S. Araújo, M. F. G. Pereira, G. M. G. da Silva, G. F. Tavares, C. Y. B. Oliveira and P. M. Faia, *Toxics*, 2023, **11**(8), 658.
5 S. E. Kim, H. J. Yang, S. Choi, E. Hwang, M. Kim, H. J. Paik, J. E. Jeong, Y. Il Park, J. C. Kim, B. S. Kim and S. H. Lee, *Green Chem.*, 2022, **24**, 251–258.
6 B. Ramesh Naidu and K. Venkateswarlu, *Green Chem.*, 2022, **24**, 6215–6223.
7 S. Maddila, O. A. Abafe, H. N. Bandaru, S. N. Maddila, P. Lavanya, N. Seshadri and S. B. Jonnalagadda, *Arab. J. Chem.*, 2019, **12**, 3814–3824.
8 X. H. Chen, X. Y. Xu, H. Liu, L. F. Cun and L. Z. Gong, *J. Am. Chem. Soc.*, 2006, **128**, 14802–14803.
9 Y. Li, T. Tan, Y. Zhao, Y. Wei, D. Wang, R. Chen and L. Tao, *ACS Macro Lett.*, 2020, **9**, 1249–1254.
10 M. Marinescu, *Molecules*, 2021, **26**, 1–34.
11 S. M. Rida, S. A. M. El-Hawash, H. T. Y. Fahmy, A. A. Hazzaa and M. M. M. El-Meligy, *Arch. Pharm. Res.*, 2006, **29**, 826–833.
12 M. H. El-Wakil, M. Teleb, M. M. Abu-Serie, S. Huang, G. W. Zamponi and H. Fahmy, *Bioorg. Chem.*, 2021, **115**, 105262.
13 A. Singadi, K. Venkateswarlu and I. J. Adv, *Pharm. Biotechnol.*, 2020, **6**, 4–9.
14 M. A. M. Abdel Reheim, I. S. Abdel Hafiz and H. S. E. Abdel Rady, *Mol. Divers.*, 2022, **26**, 741–755.
15 N. C. Desai, G. M. Kotadiya, K. A. Jadeja, K. N. Shah, A. H. Malani, V. Manga and T. Vani, *Bioorg. Chem.*, 2021, **115**, 105173.
16 N. Afradi, N. Foroughifar, H. Pasdar and M. Qomi, *Res. Chem. Intermed.*, 2019, **45**, 3251–3271.
17 V. Sharma, S. K. Gupta and M. Verma, *Cancer Chemother. Pharmacol.*, 2019, **84**, 1157–1166.
18 K. M. Bairagi, N. S. Younis, P. M. Emeka, K. N. Venugopala, O. I. Alwassil, H. E. Khalil, E. Sangtani, R. G. Gonnade, V. Mohanlall and S. K. Nayak, *J. Mol. Struct.*, 2021, **1227**, 129412.
19 O. Alam, S. A. Khan, N. Siddiqui, W. Ahsan, S. P. Verma and S. J. Gilani, *Eur. J. Med. Chem.*, 2010, **45**, 5113–5119.
20 M. Teleb, F. X. Zhang, J. Huang, V. M. Gadotti, A. M. Farghaly, O. M. AboulWafa, G. W. Zamponi and H. Fahmy, *Bioorganic Med. Chem.*, 2017, **25**, 1926–1938.

21 C. G. Neochoritis, T. Zarganes-Tzitzikas, C. A. Tsoleridis, J. Stephanidou-Stephanatou, C. A. Kontogiorgis, D. J. Hadjipavlou-Litina and T. Choli-Papadopoulou, *Eur. J. Med. Chem.*, 2011, **46**, 297–306.
22 R. E. Ferraz de Paiva, E. G. Vieira, D. Rodrigues da Silva, C. A. Wegermann and A. M. Costa Ferreira, *Front. Mol. Biosci.*, 2021, **7**, 1–24.
23 G. Singh, P. Kalra, A. Singh, G. Sharma, P. Sanchita, Mohit, C. Espinosa-Ruíz and M. A. Esteban, *J. Organomet. Chem.*, 2021, **953**, 122051.
24 S. Nain, G. Mathur, T. Anthwal, S. Sharma and S. Paliwal, *Pharm. Chem. J.*, 2023, **57**, 196–203.
25 V. K. R. Tangadanchu, Y. F. Sui and C. H. Zhou, *Bioorganic Med. Chem. Lett.*, 2021, **41**, 128030.
26 Y. Q. Hu, S. Zhang, F. Zhao, C. Gao, L. S. Feng, Z. S. Lv, Z. Xu and X. Wu, *Eur. J. Med. Chem.*, 2017, **133**, 255–267.
27 D. Sriram, P. Yogeeswari and K. Meena, *Pharmazie*, 2006, **61**, 274–277.
28 X. H. Makhoba, C. Viegas, R. A. Mosa, F. P. D. Viegas and O. J. Pooe, *Drug Des. Devel. Ther.*, 2020, **14**, 3235–3249.
29 A. Bastero, D. Font and M. A. Pericàs, *J. Org. Chem.*, 2007, **72**, 2460–2468.
30 R. Kharb, P. C. Sharma and M. S. Yar, *J. Enzyme Inhib. Med. Chem.*, 2011, **26**, 1–21.
31 T. A. Wani, N. Alsaif, M. M. Alanazi, A. H. Bakheit, S. Zargar and M. A. Bhat, *Eur. J. Pharm. Sci.*, 2021, **158**, 105686.
32 A. Mushtaq, R. Asif, W. A. Humayun and M. M. Naseer, *RSC Adv.*, 2024, **14**, 14051–14067.
33 E. D. Dalvie, J. C. Stacy, K. C. Neuman and N. Osheroff, *Biochemistry*, 2022, **61**, 2148–2158.
34 A. J. Lang, S. E. L. Mirski, H. J. Cummings, Q. Yu, J. H. Gerlach and S. P. C. Cole, *Gene*, 1998, **221**, 255–266.
35 J. L. Delgado, C. M. Hsieh, N. L. Chan and H. Hiasa, *Biochem. J.*, 2018, **475**, 373–398.
36 A. Ismail, A. S. Doghish, B. E. M. Elsadek, S. A. Salama and A. D. Mariee, *Steroids*, 2020, **160**, 108656.
37 J. Cortés, S.-B. Kim, W.-P. Chung, S.-A. Im, Y. H. Park, R. Hegg, M. H. Kim, L.-M. Tseng, V. Petry, C.-F. Chung, H. Iwata, E. Hamilton, G. Curigliano, B. Xu, C.-S. Huang, J. H. Kim, J. W. Y. Chiu, J. L. Pedrini, C. Lee, Y. Liu, J. Cathcart, E. Bako, S. Verma and S. A. Hurvitz, *N. Engl. J. Med.*, 2022, **386**, 1143–1154.
38 H. A. Bashmail, A. A. Alamoudi, A. Noorwali, G. A. Hegazy, G. M. Ajabnoor and A. M. Al-Abd, *Molecules*, 2020, **25**, 2–15.
39 V. Jain, H. Kumar, H. V. Anod, P. Chand, N. V. Gupta, S. Dey and S. S. Kesharwani, *J. Control. Release*, 2020, **326**, 628–647.
40 P. K. Mishra, P. Gahlyan, R. Kumar and P. K. Rai, *ACS Sustain. Chem. Eng.*, 2018, **6**, 10668–10678.
41 K. N. Venugopala, R. Govender, M. A. Khedr, R. Venugopala, B. E. Aldhubiab, S. Harsha and B. Odhav, *Drug Des. Devel. Ther.*, 2015, **9**, 911–921.
42 K. Bhagat, J. Bhagat, M. K. Gupta, J. V. Singh, H. K. Gulati, A. Singh, K. Kaur, G. Kaur, S. Sharma, A. Rana, H. Singh, S. Sharma and P. M. S. Bedi, *ACS Omega*, 2019, **4**, 8720–8730.
43 V. Castro, H. Rodríguez and F. Albericio, *ACS Comb. Sci.*, 2016, **18**, 1–14.
44 S. Kaur, J. Kaur, B. A. Zarger, N. Islam and N. Mir, *Heliyon*, 2024, **10**, e35897.
45 V. C. Jordan, *Nat. Rev. Drug Discovery*, 2003, **2**, 205–213.